Facile Layer Diffusion Technique for Synthesis of Terbium-Based Metal Organic Framework for Fluorometric Sensing of Hydroquinone

Gurdeep Singh
Punjabi University
Rajpal Verma
Punjabi University
Kirandeep Kaur
Punjabi University
Deepika -
Punjabi University
Sanjay Kumar
Multani Mal Modi College
Ashok Kumar Malik
malik_chem2002@yahoo.co.uk

Punjabi University

Research Article

Keywords: Metal organic framework, Layer diffusion technique, Morphology, Hydroquinone, p-Benzoquinone, Fluorescence sensing, Turn-off quenching

Posted Date: February 1st, 2024

DOI: https://doi.org/10.21203/rs.3.rs-3894601/v1

Additional Declarations: No competing interests reported.

Version of Record: A version of this preprint was published at Journal of Fluorescence on April 9th, 2024.
See the published version at https://doi.org/10.1007/s10895-024-03682-0.

Facile Layer Diffusion Technique for Synthesis of Terbium-Based Metal Organic Framework for Fluorometric Sensing of Hydroquinone

Gurdeep Singh [a], Rajpal Verma [a,c], Kirandeep Kaur [a], Deepika [a], Sanjay Kumar [b], Ashok Kumar Malik [a *]

[a] *Department of Chemistry, Punjabi University, Patiala-147002, Punjab, India*

[b] *Department of Chemistry, Multani Mal Modi College, Patiala-147001, Punjab, India*

[c] *Department of Chemistry, Dr. B. R. Ambedkar Govt. College Dabwali, Sirsa, Haryana, India*

[*]Corresponding author: malik_chem2002@yahoo.co.uk (A.K.M.)

ABSTRACT

A photoluminescent terbium(III)-based Metal Organic Framework (MOF) was synthesized at room temperature by layer diffusion method utilising mixed carboxylate linkers (4,4'-oxybis(benzoic acid) and benzene-1,3,5 tricarboxylic acid). Synthesized MOF has crystalline nature and rod-shaped morphology and is thermally stable up to 455°C. From elemental analysis, Carbon, oxygen, and terbium were all found to be present in the synthesized MOF. The fluorescence emission spectra and theoretical results revealed that carboxylate linkers functioned as sensitizers for Tb(III) photoluminescence which resulted in four distinct emission peaks at 495, 547, 584, and 621 nm corresponding to the transitions $^5D_4 \rightarrow {}^7F_6$, $^5D_4 \rightarrow {}^7F_5$, $^5D_4 \rightarrow {}^7F_4$, and $^5D_4 \rightarrow {}^7F_3$. Using synthesized MOF as fluorescent probe, hydroquinone was detected in aqueous medium with a detection limit of 0.048 μM, remarkable recovery (95.6-101.1%), and relative standard deviation less than 2.25%. The quenching phenomenon may be ascribed by electron transfer from synthesized probe to oxidized hydroquinone via carboxylic groups on the surface of MOF, which is further supported by photo-induced electron transfer mechanism. This study introduces a cheaper, faster, and more accurate method for hydroquinone detection.

Keywords: *Metal organic framework, Layer diffusion technique, Morphology, Hydroquinone, p-Benzoquinone, Fluorescence sensing, Turn-off quenching.*

Highlights

- Layer diffusion method has been used to synthesize MOF (**PUP-1**).
- Synthesized MOF exhibits excellent sensitivity for HQ detection (LOD = 0.048 μM).
- **PUP-1** has high ability of reusability without noticeable decrease in sensitivity.
- The transfer of electrons between probe and analyte is responsible for fluorescence quenching.

Graphical Abstract

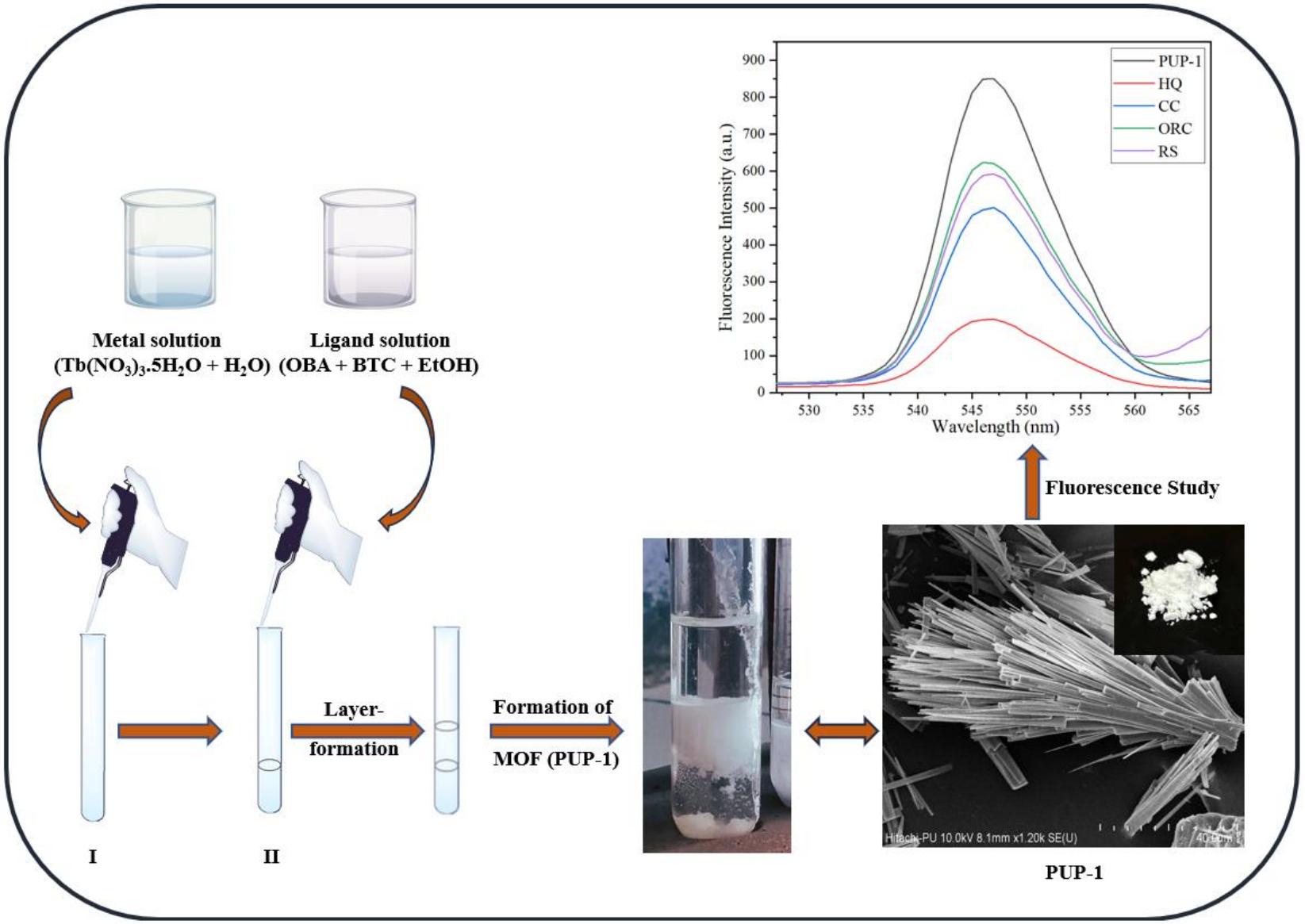

1. Introduction

The study and detection of phenolic compounds has received a lot of attention as these compounds are common organic contaminants that are released as waste into water bodies because of their widespread usage. Hydroquinone (HQ), a common organic pollutant has been used in large-scale industrial and biological fields such as rubber anti-aging agents, anthraquinone dyes, stabilizers, antioxidants, azo dyes, white and black developers, etc [1] and its absorption is hazardous to humans and can results in death because of low degradability and severe toxic effects. The nerve centre system inhibition and incurring liver and kidney function damage caused by HQ and catechol (CC) were also reported [2, 3]. As a result, establishing an analytical approach for concurrent discrimination and quick identification of these pollutants is extreme requirement. The development of an easy and fast method for identifying isomers is an important and difficult task in biology, chemistry, pharmacology, and environmental studies due to the small differences in the skeleton of isomers and similar physical and chemical properties [4]. Therefore, such pollutant identification must be sensitive and selective. Prior research has documented several detection techniques, including electrochemiluminescence (ECL) [5], gas chromatography (GC) [6], flow injection analysis [7], voltammetry [8, 9], high-performance liquid chromatography (HPLC) [10], etc. These methods of detection have a significant advantage due to their rapid response as well as excellent sensitivity [11, 12]. However, it cannot be denied that these methods have limitations because of the expensive equipment, complicated or labour-intensive procedures. So, the fluorescence technique which is an excellent substitute for HQ identification with excellent specificity, offers unique advantages of easy monitoring, quick response, and simple and easy functioning [13].

In precise fluorescence detection of HQ, the primary step is to construct a highly selective fluorescent probe. Among the fluorescent probes, Metal organic frameworks (MOFs) have

grown in popularity and interest in recent years. The MOFs are a group of crystalline organic-inorganic hybrid compounds composed of metallic ions or assemblies that act as nodes linked by organic linkers as a bridged connection, These materials demonstrated a variety of applications in different fields, including bio-imaging [14], sensing [15], catalysis [16], magnetism [17], drug delivery [18], adsorption, gas storage/separation [19], and photocatalysis [20], showing versatile properties like large surface area and pore size distribution, lower density, well-defined crystalline structure, chemical tunability, high pore volume, and high surface to volume ratio [21, 22].

In the current study, a Tb(III) based MOF namely **PUP-1** (PUP = Punjabi University Patiala) was synthesized via simple layer diffusion method using mixed ditopic and tritopic carboxylate ligands (4,4'-oxybis(benzoic acid) (OBA) and benzene-1,3,5 tricarboxylic acid (BTC)) having different metrical parameters which modify framework topology retaining robust structure remarkably, tuning chirality, and chemical selectivity [23-26]. The developed MOF was used for selective and sensitive identification of HQ. To extent of our knowledge, this work marks the first comprehensive evaluation focused on fluorescent detection of HQ by terbium MOF (**PUP-1**). Furthermore, it was concluded that the remarkable structural stability and unique functionality of **PUP-1** make it extremely suitable for rapid and accurate detection of HQ in aqueous media. Theoretical findings reveal a strong relationship between theoretical and experimental studies. Therefore, it is anticipated that the chemical, morphological, and spectrometric properties of the synthesized materials would be better understood by the present investigation.

2. Experimental Section

2.1. Chemicals and Materials

Terbium nitrate pentahydrate ($Tb(NO_3)_3.5H_2O$), 4,4'-oxybis(benzoic acid) (OBA), benzene-1,3,5 tricarboxylic acid (BTC), hydroquinone (HQ), catechol (CC), resorcinol (RS) and orcinol (ORC) were supplied by Sigma-Aldrich (Mumbai, India). sodium hydroxide (NaOH) and hydrochloric acid (HCl), were obtained from Loba Chemie (Mumbai, India). Every reagent that was used was of analytical grade and was utilized exactly as received. Throughout the process, triply distilled water (TDW) was used.

2.2. Measurements

On a Perkin Elmer RXIFT-IR Spectrophotometer (Japan), the Fourier transform infrared (FT-IR) spectra of BTC, OBA, and PUP-1 were analysed in 450–4000 cm^{-1} range. PXRD diffractograms were obtained for the purpose of determining the crystalline structure using Panalytical's X'Pert Pro Power X-ray Diffractometer [CuKα X-ray (λ=1.54Å), 45 kV, and 40 mA]. The morphology and topography of the synthesized MOF were examined using a Hitachi SU8010 Series (Japan) Field Emission Scanning Electron Microscope (FE-SEM). The EDX spectrum was obtained using an energy-dispersive X-ray (EDX) spectrometer that was provided as an additional FE-SEM equipment (Hitachi SU8010 Series, Japan), fixed properly on the specimen's stub. On a Hitachi STA7300 (Japan) with a temperature range of 35°C to 800°C (rate of heating =10°C/min) and a pure nitrogen environment, thermogravimetric analysis (TGA) was carried out. Studies of photoluminescence (PL) and absorbance spectra were conducted using a Shimadzu RF-5301PC spectrofluorometer (Japan) and Shimadzu UV–Vis 1600 spectrophotometer respectively.

2.3. General Procedure for the synthesis of **PUP-1***:*

Initially, BTC (42 mg, 0.2 mmol) and OBA (77 mg, 0.3 mmol) were dissolved in 20 ml of ethanol to prepare ligand solution and $Tb(NO_3)_3.5\ H_2O$ (87 mg, 0.2 mmol) was dissolved in 20 ml of water to produce the metal solution. Both solutions were subjected to a 10 min sonication

process. Subsequently, a glass test tube was filled with 2 mL of the metal solution. Following that, 2 mL of the ligand solution was carefully added around the inner sides of the tube, creating a layer between the ligand and metal solutions. Test tube was then left undisturbed for 1 week at room temperature. In the region of the middle layer, white crystalline solid MOF particles were accumulated. After centrifugation at 8000 rpm for 8 min and three times washing with 5 mL of each ethanol and water separately, the final product (**PUP-1**) was obtained. Finally, the crystals of **PUP-1** were dried and placed in a desiccator to keep them moisture-free until they were used in PL sensing analysis.

2.4. Sample preparation for PL analysis

Since **PUP-1** exhibits outstanding dispersion and strong aqueous media stability, water was selected as the solvent to investigate PL measurements of **PUP-1** toward distinct isomeric benzenediols (HQ, CC, RS and ORC). To prepare a stock suspension for PL measurement, 1 mg of **PUP-1** was dispersed in deionized water (100 mL) and subjected to a 15-minute sonication. Analytical standard aqueous solutions (0.4 μM) of isomeric benzenediols were also prepared in water. To conduct the selective PL analysis, analyte solution (2.8 mL) was mixed with the stock suspension of **PUP-1** (0.2 mL) to make total volume of 3 mL. In order to achieve enhanced analyte detection, the experimental parameters such as pH and the response time, were optimized. Throughout PL investigations, the excitation wavelength (λ_{ex}) and slit width (excitation and emission monochromators) were kept at 272 nm and 5 nm, respectively.

3. Results and Discussion

3.1. Characterization of PUP-1

3.1.1. FT-IR

FT-IR spectra of **PUP-1**, OBA, and BTC are illustrated in Figure 1. For non-ionized BTC and OBA, the C=O stretching vibrations appeared at 1694 cm^{-1} and 1677 cm^{-1} respectively and C-

O stretching vibrations observed at 1265 cm^{-1} and 1250 cm^{-1} respectively. After formation of MOF, the appearance of symmetric and asymmetric stretching vibrations of carboxylate groups (from OBA and BTC) at 1409 cm^{-1} and 1546 cm^{-1} respectively indicate successful coordination of linkers with terbium ions [27]. Also, the stretching bands of aromatic C-H, aromatic C=C and Tb-O bend have been found at 3070 cm^{-1}, 1607 cm^{-1} and 530 cm^{-1} respectively for synthesized MOF [28].

3.1.2. PXRD

PXRD was used to explore diffraction patterns of **PUP-1**. Diffraction patterns recorded at 2θ for synthesized **PUP-1** validates the crystalline structure. At 2θ = 16.24° in the hkl plane (100), the maximum intensity of diffraction peak was noted (Figure 2). Other peaks were displayed in the recorded PXRD diffractograms at 10.92°, 11.93°, 14.67°, 19.82°, 20.67°, 22.51°, 25.63°, 26.90°, 28.43°, 29.53°, 34.56°, and 38.20°, with corresponding to the planes (010), (001), (010), (110), (101), (111), (200), (020), (002), (210), (211), and (220) respectively, indicating the crystallinity of the synthesized **PUP-1** [27, 29].

3.1.3. TGA

The stability of synthesized compound (**PUP-1**) with temperature was investigated by the TGA (Figure 3). The first resulting curve indicates a reduction of about 22.42% within the 215–315°C range of temperature, that is associated with the de-solvation and dehydration processes. The solvent moieties trapped within the pores of **PUP-1** are lost in the temperature range previously mentioned. The complete breakdown of framework and disintegration of the MOF linkers cause second curve to appear after 455°C. This curve clearly shows that **PUP-1** remained stable until it approached 455°C, after that a faster weight loss of about 39.69% occurred, indicating collapse of MOF structure.

3.1.4. FE-SEM

FE-SEM was applied to investigate the structural and topographical morphology of **PUP-1**. FE-SEM micrographs at magnifications of x1,200 and x2,200 is shown in Figure 4. These micrographs demonstrate that the synthesized MOF has a rod-shaped morphology. Along with this, most of the rods have widths between 0.80 to 1.40 μm, which resulted in average width of 1.18 μm (Figure S1).

3.1.5. EDX and Mapping

According to compositional analysis of EDX spectra, **PUP-1** contains carbon (C), oxygen (O), and terbium (Tb), with detected weight (atomic) percent of 26.08% (54.45%), 24.03% (37.67%), and 49.89% (7.87%), respectively (Figure S2). By showing the presence of organic linkers and metal ions, EDX analysis affirmed the high-purity MOF formation. The elemental mapping of O, C, and Tb is shown in Figure S3. The presence of all elements in **PUP-1** with appropriate stoichiometric ratios was demonstrated by both the mapping investigation and the EDX spectra, confirming the high-purity MOF formation.

3.2. PL study

The excitation spectrum (λ_{em}= 547 nm) of the synthesized **PUP-1** has shown two distinct humps in the range of 225–325 nm (Figure 5a). These humps are associated with charge-transfer mechanism between the oxygen and terbium ions along with π–π* electron transitions of the organic ligands [28, 30]. Figure 5b displays the emission spectrum (λ_{ex} = 272 nm) of **PUP-1** dispersed in aqueous medium. The Tb^{3+} ion exhibits distinctive transitions at 495, 547, 584, and 621 nm, which are assigned as $^5D_4 \rightarrow {}^7F_6$, $^5D_4 \rightarrow {}^7F_5$, $^5D_4 \rightarrow {}^7F_4$, and $^5D_4 \rightarrow {}^7F_3$ respectively [31, 32].

3.2.1. pH effect and response time

The PL spectra of probe-analyte system were examined in pH range of 4 to 8.5 using solutions of NaOH (0.2 M) and HCl (0.2 M). At various pH levels, the fluorescence intensity of **PUP-1**

and **PUP-1** + HQ was measured. The PL intensity of **PUP-1** does not change significantly within the pH range of 4–8.5. The **PUP-1** + HQ system showed a decrease in fluorescence in alkaline media, but a higher platform of fluorescence intensity in acidic and neutral solutions (Figure S4(a)). When HQ was added at a pH of 8, the fluorescence emission intensity was at its lowest. Thus, pH 8 was chosen as best pH level for PL experiments [33]. Further to perform the time-dependent detection of HQ, the emission spectra of the **PUP-1** + HQ suspension at pH 8 were observed at 1 min intervals to up to 10 min. Figure S4(b) demonstrates that the fluorescence intensity of MOF remains constant for duration of 2-10 min. The optimal response time, therefore, is determined to be 2 min.

3.2.2. Detection of HQ

The PL emission spectra (λ_{ex} = 272 nm) of each mixture (**PUP-1**+ analyte) were investigated and compared to perform a selective analysis (Figure 6). It is noteworthy that while other isomeric benzenediols (CC, RS, and ORC) showed a minor to moderate quenching in PL emission intensity, the luminescence was significantly quenched by HQ. These findings suggest that the **PUP-1** can identify HQ in an aqueous solution with good selectivity.

Further, the impact of HQ on PL emission intensity was measured to examine the sensitivity of **PUP-1** (Figure 7). Surprisingly, PL emission intensity dropped with increase in HQ concentration. The molar concentration of the analyte (C) and relative fluorescence intensity (F_0/F) have a linear relationship, according to the Stern-Volmer (SV) equation expressed as $F_0/F-1= K_{SV}\times[C]$, where F_0 and F stand for PL emission intensity values for **PUP-1** before and after the addition of HQ respectively, and K_{SV} denotes Stern-Volmer constant (M^{-1}) [34]. The SV plot was found to be linear up to 0.225 μM (Figure 8). By use of formula; LOD = 3.3 σ/m, where 'σ' denotes linear curve standard deviation (SD) and 'm' denotes its slope, the LOD of **PUP-1** for HQ was found to be 0.048 μM in an aqueous medium. In comparison to previously

169 published techniques, the detection efficiency of synthesized MOF was also evaluated. Table
170 1 demonstrates that **PUP-1** has shown an excellent lower value of LOD (0.048 μM) for
171 detection of HQ compared with other stated materials and techniques.

172 ***3.2.3. Recyclability***

173 After third sensing cycle, fluorescence properties of recovered probe (**PUP-1**) were observed.
174 It was found that, the quenching efficiency of MOF stayed essentially the same until the third
175 recycling cycle. The chemical and mechanical stability of **PUP-1** was demonstrated by the fact
176 that the addition of HQ did not change its PXRD pattern and FT-IR spectrum (Figure S5).
177 These outcomes showed that synthesized MOF has outstanding stability in aqueous media and
178 recyclability for up to third cycle.

179 ***3.2.4. Mechanism***

180 To further understand the detailed mechanism of the quenching phenomenon, the interactions
181 of **PUP-1** with HQ were examined. The different charge densities on isomeric benzenediols
182 and electron transfer between probe and analyte are possible reasons for PL quenching.

183 In alkaline solution, HQ is rapidly oxidized (into p-benzoquinone (BQ)) in comparison to other
184 isomers because they are relatively more stable than HQ. The hydroxyl functional groups on
185 benzene of HQ, CC, and RS (or ORC) are not at same position relative to each other. This
186 means that the charge density is not distributed in the same way. When both hydroxyl groups
187 are in opposing positions, the charge density is highest. As high charge density makes HQ more
188 susceptible to be oxidised, it functions as good electron acceptor [35-37]. The different
189 electron-accepting powers of isomeric benzenediols leads to different rates of electron transfer,
190 which results in greatest selectivity of **PUP-1** for HQ. So, we propose that decrease of
191 fluorescence intensity is caused by electron transfer from photo excited **PUP-1** to BQ
192 via carboxylic groups as shown in Figure 9 [38]. Further, to support above discussed electron

transfer phenomenon between probe and analyte, the photo-induced electron transfer (PET) mechanism was studied [39, 40]. The energy levels of **PUP-1** linkers (OBA and BTC) and BQ were calculated by B3LYP/6-311G basic set and Gaussian 09 package. The lowest unoccupied molecular orbital (LUMO) of BQ is located in between valence bands and conduction bands of **PUP-1** ligands (Figure 10). Consequently, the transfer of electrons to LUMO of BQ from conduction band of **PUP-1** is relatively fast than de-excitation of conduction band to valence band. In contrast to higher energetic LUMO of MOF, BQ having LUMO close to its valence band is better option for acceptance of electrons, which results in high quenching performance.

3.2.5. Practicability

Experiments were conducted by spiking HQ into tap and river water, to examine the practicability of established method for environmental samples. The recoveries that range from 95.6 to 101.1 % were noticed, with a maximum RSD of 2.19% (Table 2). The precise results and excellent recovery suggest that method can potentially be used to detect HQ in environmental samples.

4. Conclusion

The photoluminescent MOF (**PUP-1**) synthesized by facile layer diffusion technique was employed to develop an effective HQ sensing method showing great quenching efficiency in aqueous media. The synthesized MOF exhibited lower detection limit of 0.048 μM, thereby establishing its efficacy as a great sensor for HQ detection. The affordability, rapidity, recyclability, and excellent sensitive nature of **PUP-1** make it a potentially effective material for rapid HQ detection. The developed MOF is applicable to real aqueous samples for real-time applications of HQ residue determinations. These promising results will facilitate future research into innovative materials that could be utilized to identify HQ in environmental samples in a targeted and sensitive manner.

Acknowledgments

One of the authors, Gurdeep Singh, is grateful to University Grants Commission (UGC), New Delhi, India, for providing a junior research fellowship. We are highly thankful to RSIC, Panjab University, Chandigarh, and the Department of Chemistry, Punjabi University, Patiala for spectroscopic analysis.

Declarations

Author Contributions

Gurdeep Singh, Rajpal Verma, Kirandeep Kaur has performed the experiment and written the paper. Deepika and Sanjay Kumar has helped in writing the paper Ashok Kumar Malik has edited the paper and supervised the work. All authors have reviewed the manuscript.

Funding

No funding was available supporting this research.

Competing Interests

"The authors have no relevant financial or non-financial interests to disclose."

Data Availability

All relevant data will be provided on request.

Ethics approval

There is no ethical approval required.

Consent to participate

All authors have given consent to participate in publication process of this paper.

Consent to publish

All authors give consent to publish the paper.

References

1. Li, J., C.-y. Liu, and C. Cheng, *Electrochemical detection of hydroquinone by graphene and Pt-graphene hybrid material synthesized through a microwave-assisted chemical reduction process.* Electrochimica acta, 2011. **56**(6): p. 2712-2716.
2. Zhao, G., et al., *Electrocatalytic redox of hydroquinone by two forms Of L-proline.* Journal of Molecular Catalysis A: Chemical, 2006. **255**(1-2): p. 86-91.
3. Ahammad, A.S., et al., *Simultaneous determination of hydroquinone and catechol at an activated glassy carbon electrode.* Electroanalysis: An International Journal Devoted to Fundamental and Practical Aspects of Electroanalysis, 2010. **22**(6): p. 694-700.

4. Wang, F., Y. Yang, and T.M. Swager, *Molecular recognition for high selectivity in carbon nanotube/polythiophene chemiresistors.* Angewandte Chemie, 2008. **120**(44): p. 8522-8524.
5. Lu, Q., et al., *An electrogenerated chemiluminescence sensor based on gold nanoparticles@ C60 hybrid for the determination of phenolic compounds.* Biosensors and Bioelectronics, 2014. **60**: p. 325-331.
6. Sharma, C., et al., *Gas chromatographic determination of pollutants in the chlorination and caustic extraction stage effluent from the bleaching of a bamboo pulp.* Talanta, 1997. **44**(10): p. 1911-1918.
7. Rueda, M., et al., *Optimisation of a flow injection system with electrochemical detection using the desirability function: application to the determination of hydroquinone in cosmetics.* Analytica Chimica Acta, 2003. **479**(2): p. 173-184.
8. Velmurugan, M., et al., *Electrochemical preparation of activated graphene oxide for the simultaneous determination of hydroquinone and catechol.* Journal of colloid and interface science, 2017. **500**: p. 54-62.
9. Jiang, H., et al., *Graphene-like carbon nanosheets as a new electrode material for electrochemical determination of hydroquinone and catechol.* Talanta, 2017. **164**: p. 300-306.
10. Wittig, J., S. Wittemer, and M. Veit, *Validated method for the determination of hydroquinone in human urine by high-performance liquid chromatography–coulometric-array detection.* Journal of Chromatography B: Biomedical Sciences and Applications, 2001. **761**(1): p. 125-132.
11. Wu, X.J., M.M. Choi, and X.M. Wu, *An organic-phase optical phenol biosensor coupling enzymatic oxidation with chemical reduction.* Analyst, 2004. **129**(11): p. 1143-1149.
12. Paranjpe, P., et al., *A disposable optrode using immobilized tyrosinase films.* Analytical biochemistry, 2001. **294**(2): p. 102-107.
13. Wang, Y., et al., *Fluorometric determination of hydroquinone by using blue emitting N/S/P-codoped carbon dots.* Microchimica Acta, 2018. **185**: p. 1-9.
14. Wang, H.-S., *Metal–organic frameworks for biosensing and bioimaging applications.* Coordination Chemistry Reviews, 2017. **349**: p. 139-155.
15. Achmann, S., et al., *Metal-organic frameworks for sensing applications in the gas phase.* Sensors, 2009. **9**(3): p. 1574-1589.
16. Lee, J., et al., *Metal–organic framework materials as catalysts.* Chemical Society Reviews, 2009. **38**(5): p. 1450-1459.
17. Humphrey, S.M. and P.T. Wood, *Multiple areas of magnetic bistability in the topological ferrimagnet [Co3 (NC5H3 (CO2) 2-2, 5) 2 (μ3-OH) 2 (OH2) 2].* Journal of the American Chemical Society, 2004. **126**(41): p. 13236-13237.
18. Horcajada, P., et al., *Porous metal–organic-framework nanoscale carriers as a potential platform for drug delivery and imaging.* Nature materials, 2010. **9**(2): p. 172-178.
19. Al-Kutubi, H., et al., *Electrosynthesis of metal–organic frameworks: challenges and opportunities.* ChemElectroChem, 2015. **2**(4): p. 462-474.
20. Zhang, T. and W. Lin, *Metal–organic frameworks for artificial photosynthesis and photocatalysis.* Chemical Society Reviews, 2014. **43**(16): p. 5982-5993.
21. Caskey, S.R. and A.J. Matzger, *Selected Applications of Metal-Organic Frameworks in Sustainable Energy Technologies||.* Mater. Matters, 2009. **4**: p. 111.
22. Lu, W., et al., *Tuning the structure and function of metal–organic frameworks via linker design.* Chemical Society Reviews, 2014. **43**(16): p. 5561-5593.
23. Zhao, X.-L. and W.-Y. Sun, *The organic ligands with mixed N-/O-donors used in construction of functional metal–organic frameworks.* CrystEngComm, 2014. **16**(16): p. 3247-3258.
24. Pang, Q., B. Tu, and Q. Li, *Metal–organic frameworks with multicomponents in order.* Coordination Chemistry Reviews, 2019. **388**: p. 107-125.
25. Sun, C.-Y., et al., *Assembly and upconversion luminescence of lanthanide–organic frameworks with mixed acid ligands.* Inorganica Chimica Acta, 2009. **362**(2): p. 325-330.

26. Chen, W., et al., *Photoluminescent metal− organic polymer constructed from trimetallic clusters and mixed carboxylates.* Inorganic chemistry, 2003. **42**(4): p. 944-946.
27. Renata, Ł., *Hydrothermal synthesis, thermal and luminescent investigations of lanthanide (III) coordination polymers based on the 4, 40-oxybis (benzoate) ligand.* J Therm Anal Calorim, 2012. **108**(3): p. 1101-10.
28. Feng, L., et al., *Terbium-based metal-organic frameworks: Highly selective and fast respond sensor for styrene detection and construction of molecular logic gate.* Journal of hazardous materials, 2020. **388**: p. 121816.
29. Silva, I., et al., *Eu3+ or Sm3+-Doped terbium-trimesic acid MOFs: Highly efficient energy transfer anhydrous luminophors.* Optical Materials, 2018. **84**: p. 123-129.
30. Liu, K., et al., *Facile and rapid fabrication of metal–organic framework nanobelts and color-tunable photoluminescence properties.* Journal of Materials Chemistry, 2010. **20**(16): p. 3272-3279.
31. Xia, T., et al., *A terbium metal–organic framework for highly selective and sensitive luminescence sensing of Hg2+ ions in aqueous solution.* Chemistry–A European Journal, 2016. **22**(51): p. 18429-18434.
32. Campagnol, N., et al., *Luminescent terbium-containing metal–organic framework films: new approaches for the electrochemical synthesis and application as detectors for explosives.* Chemical Communications, 2014. **50**(83): p. 12545-12547.
33. Wang, M., et al., *Fluorometric assay of hydroquinone without interference from catechol and resorcinol based on carbonized polymer dots.* New Journal of Chemistry, 2023. **47**(7): p. 3462-3470.
34. Qu, B., et al., *The synthesis of porous ultrathin graphitic carbon nitride for the ultrasensitive fluorescence detection of 2, 4, 6-trinitrophenol in environmental water.* Environmental Science: Nano, 2020. **7**(1): p. 262-271.
35. He, Y., et al., *Graphene quantum dots: highly active bifunctional nanoprobes for nonenzymatic photoluminescence detection of hydroquinone.* Biosensors and Bioelectronics, 2015. **74**: p. 418-422.
36. Liu, Y., et al., *Conjugated polymer nanoparticles-based fluorescent biosensor for ultrasensitive detection of hydroquinone.* Analytica chimica acta, 2018. **1012**: p. 60-65.
37. Du, P., et al., *N-doped carbon dots from pericarpium citri reticulatae for wide linear range sensing of hydroquinone.* Fullerenes, Nanotubes and Carbon Nanostructures, 2023: p. 1-12.
38. Jaiswal, A., A. Kumar, and R. Prakash, *Facile synthesis of doped CxNy QDs as photoluminescent matrix for direct detection of hydroquinone.* Spectrochimica Acta Part A: Molecular and Biomolecular Spectroscopy, 2021. **246**: p. 119019.
39. Pramanik, S., et al., *New microporous metal− organic framework demonstrating unique selectivity for detection of high explosives and aromatic compounds.* Journal of the American Chemical Society, 2011. **133**(12): p. 4153-4155.
40. Lustig, W.P., et al., *Metal–organic frameworks: functional luminescent and photonic materials for sensing applications.* Chemical Society Reviews, 2017. **46**(11): p. 3242-3285.
41. Ni, P., et al., *Carbon dots based fluorescent sensor for sensitive determination of hydroquinone.* Talanta, 2015. **144**: p. 258-262.
42. Gao, Y., et al., *Fluorometric method for the determination of hydrogen peroxide and glucose with Fe3O4 as catalyst.* Talanta, 2011. **85**(2): p. 1075-1080.
43. Yuan, J., W. Guo, and E. Wang, *Utilizing a CdTe quantum dots− enzyme hybrid system for the determination of both phenolic compounds and hydrogen peroxide.* Analytical Chemistry, 2008. **80**(4): p. 1141-1145.
44. Liu, Y., et al., *Highly selective and sensitive fluorescence detection of hydroquinone using novel silicon quantum dots.* Sensors and Actuators B: Chemical, 2018. **275**: p. 415-421.
45. Huang, H., et al., *Water-soluble fluorescent conjugated polymer-enzyme hybrid system for the determination of both hydroquinone and hydrogen peroxide.* Talanta, 2011. **86**: p. 164-169.

Table 1. Comparative study of developed method.

381

Material used	Linear range (µM)	LOD (µM)	Ref.
CPDs	0.1- 120	0.08	[33]
Doped carbon nitride	12- 57.5	0.05	[38]
C-dots	0.1- 50	0.1	[41]
Polymer/H_2O_2-peroxidase	1- 2000	0.5	[42]
CdTeQDs-enzyme	0.5- 500	0.5	[43]
Silicon quantum dots	6- 100	2.63	[44]
$PPESO_3$-enzyme	1.0- 200	0.5	[45]
Terbium MOF (**PUP-1**)	0.05- 0.225	0.048	This work

382
383
384
385
386
387
388
389
390

391 **Table 2.** Detection of HQ in river water and tap water by **PUP-1** (n= 3).

Sample	Amount spiked (nM)	Amount found(nM)	Recovery (%)	RSD (%, n=3)
River Water	90	90.18	100.2	1.89
	150	143.9	95.9	2.12
	250	240.6	96.2	1.44
Tap Water	90	89.83	99.8	2.19
	150	151.7	101.1	2.04
	250	238.7	95.6	1.16

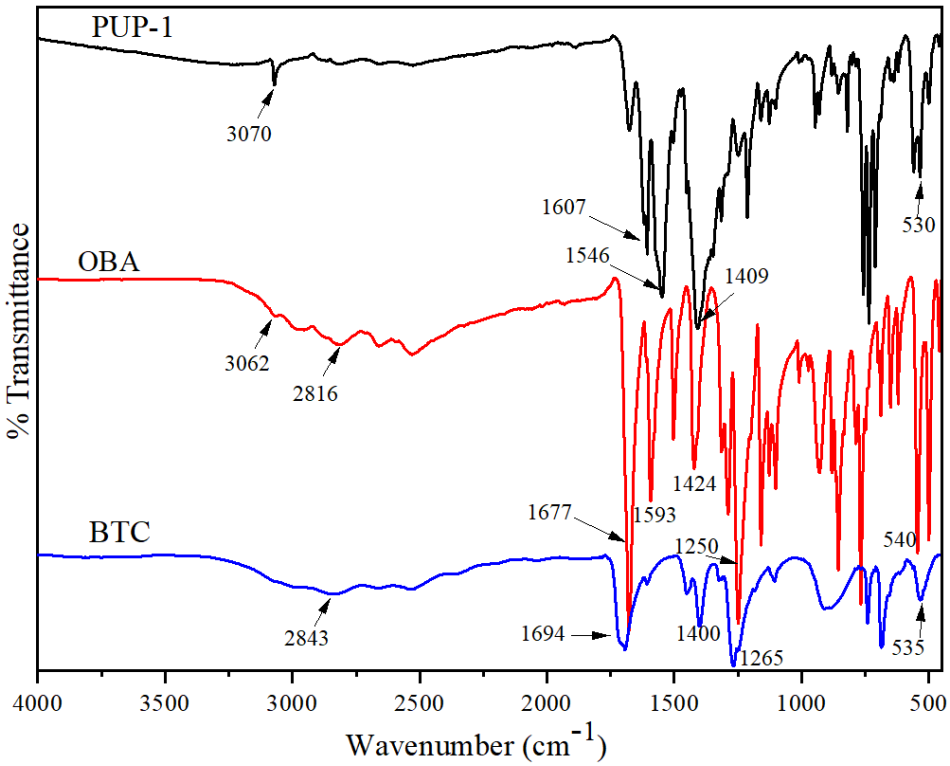

Figure 1. FT-IR spectra of **PUP-1**, OBA, and BTC.

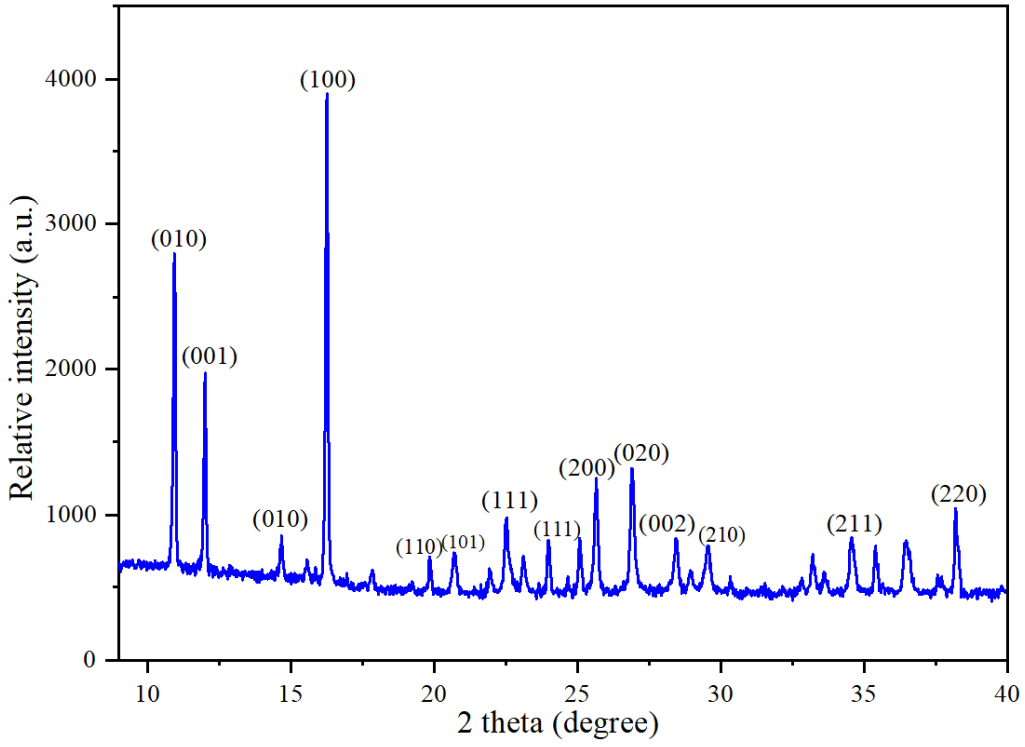

Figure 2. Powder X-ray diffractograms (PXRD) Pattern of **PUP-1**.

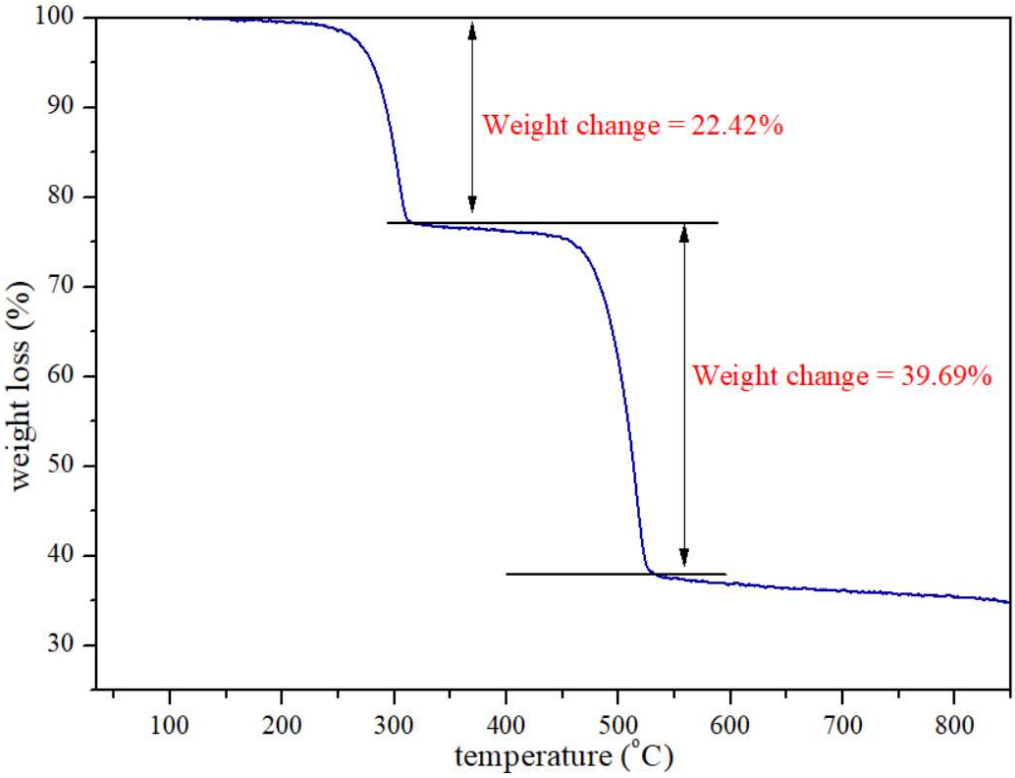

Figure 3. Thermogravimetric analysis (TGA) of **PUP-1**.

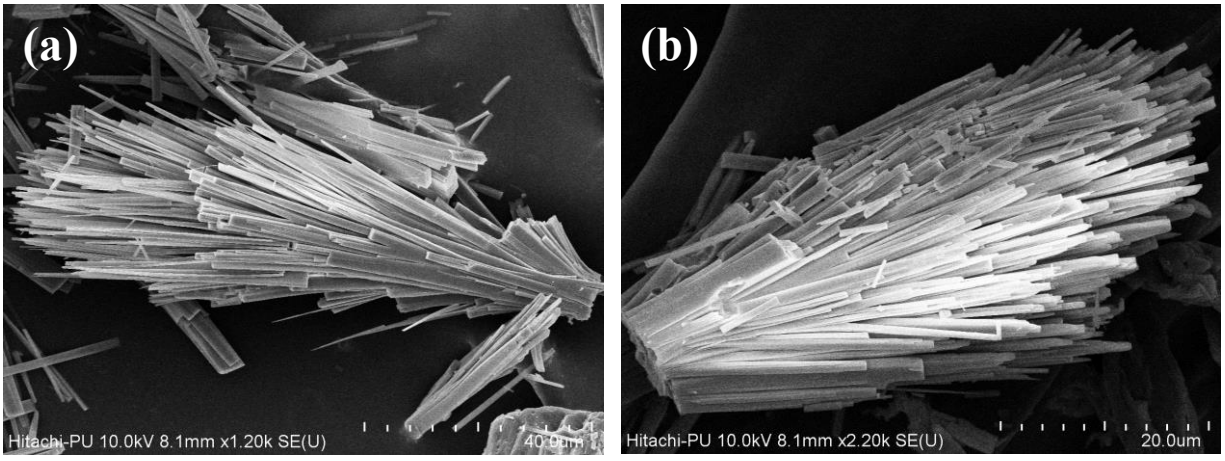

Figure 4. FE-SEM micrographs of the **PUP-1** at different magnifications **(a)** x1,200; **(b)** x2,200.

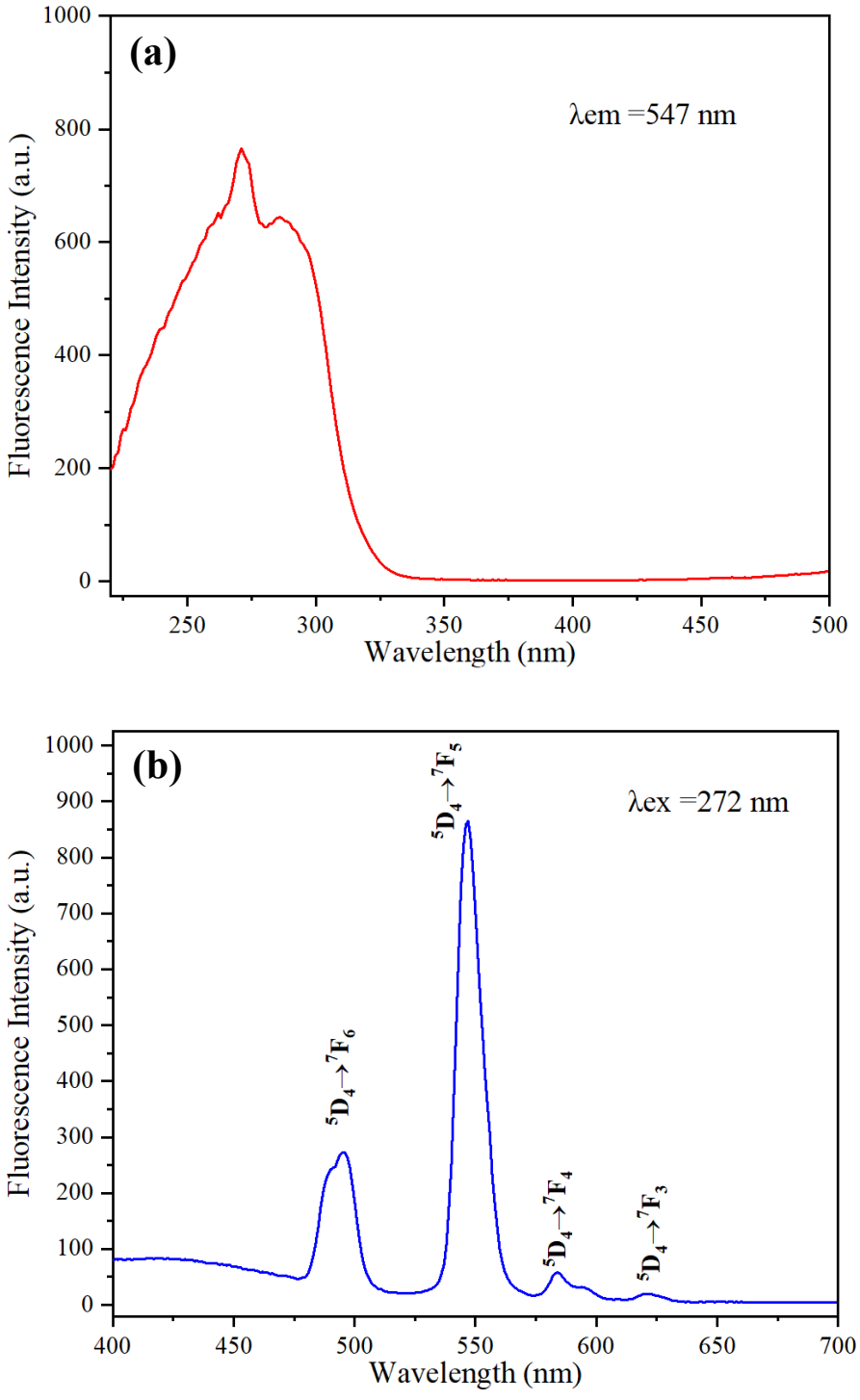

Figure 5. Excitation (a) and emission (b) spectra of the MOF (**PUP-1**).

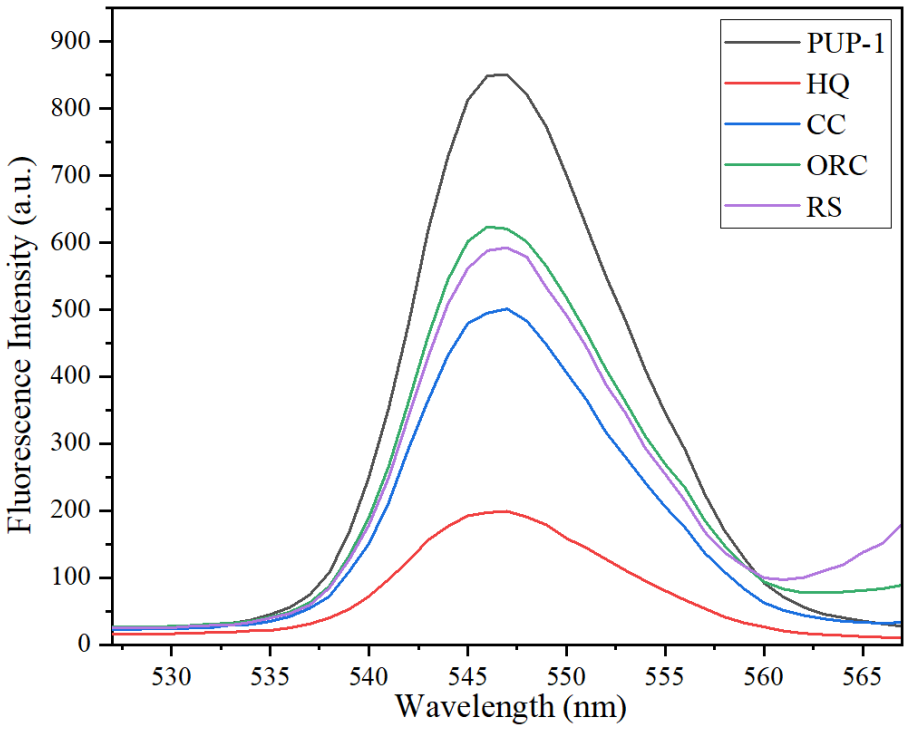

Figure 6. Fluorescence spectra of MOF (λ_{ex}= 272 nm) dispersed in aqueous solution containing HQ, CC, ORC, or RS at pH 8.

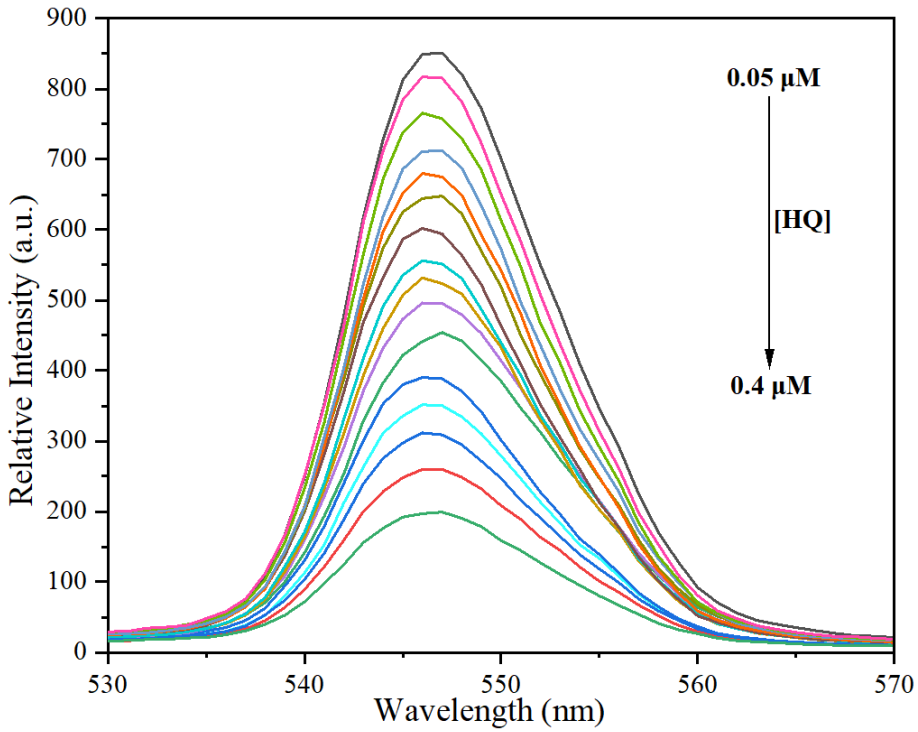

Figure 7. Quenching of fluorescence emission intensity of **PUP-1** with addition of HQ having different concentrations in the aqueous medium at pH 8.

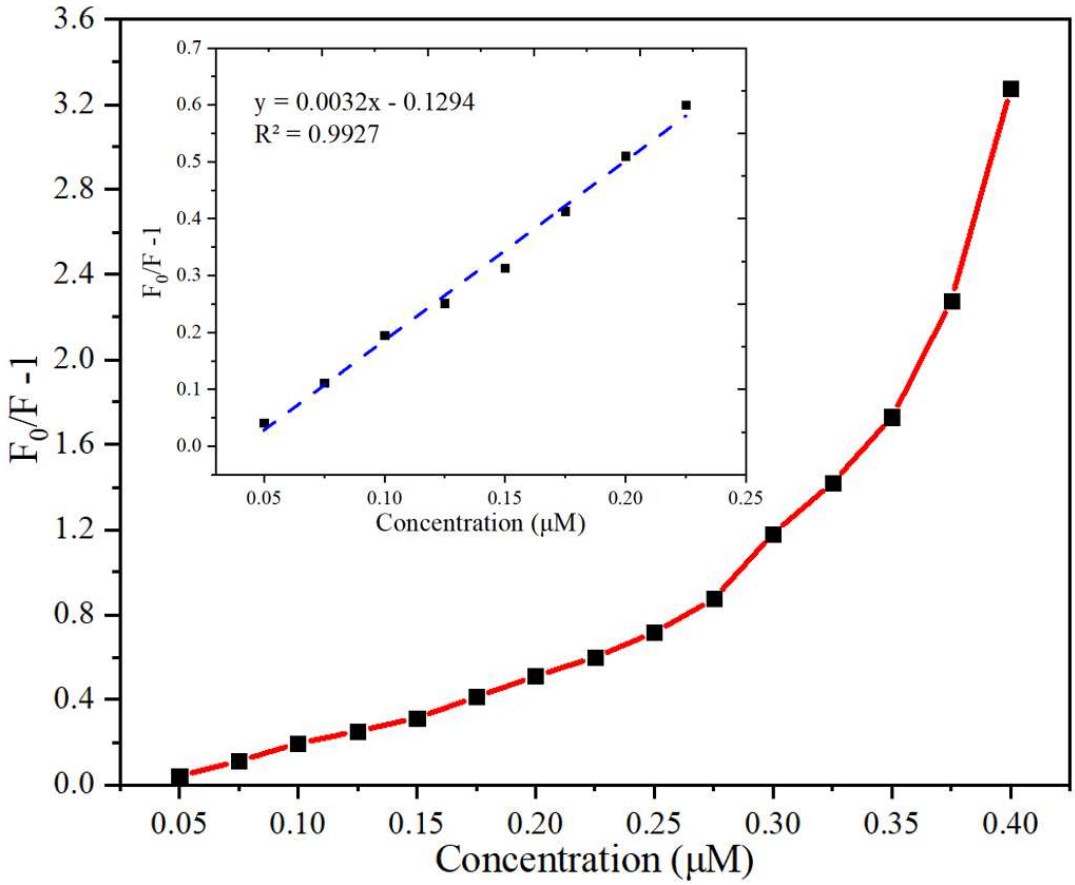

Figure 8. The stern-Volmer plot of fluorescence spectra of mixtures (**PUP-1** and HQ) at different concentrations of HQ.

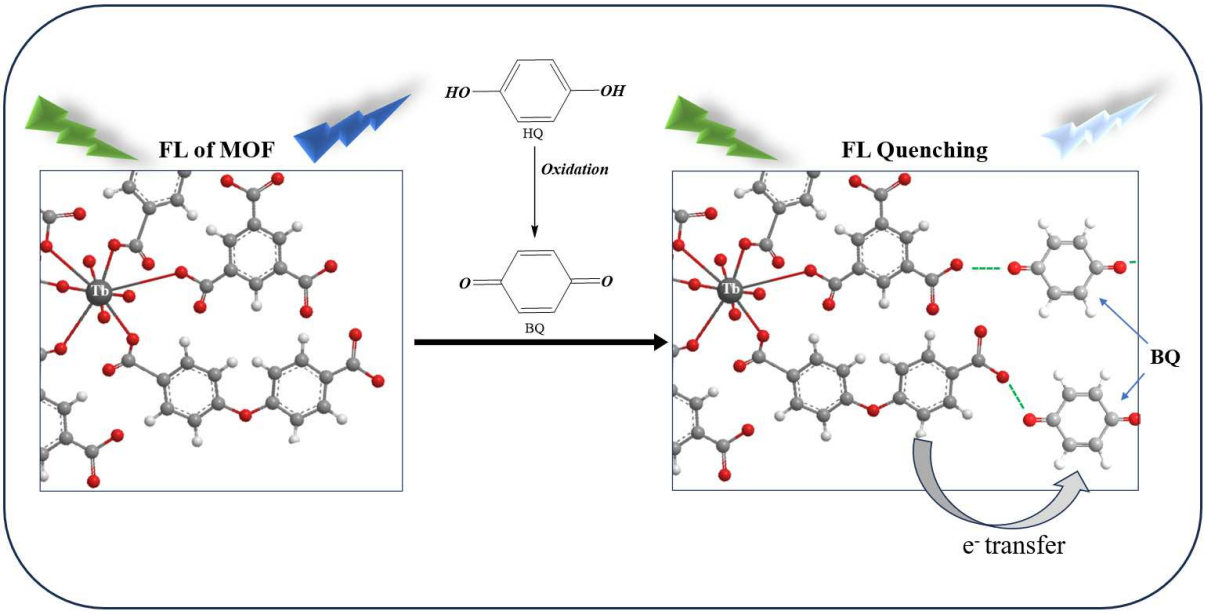

Figure 9. Schematic illustration of the possible electron transfer between developed probe (**PUP-1**) and oxidised HQ.

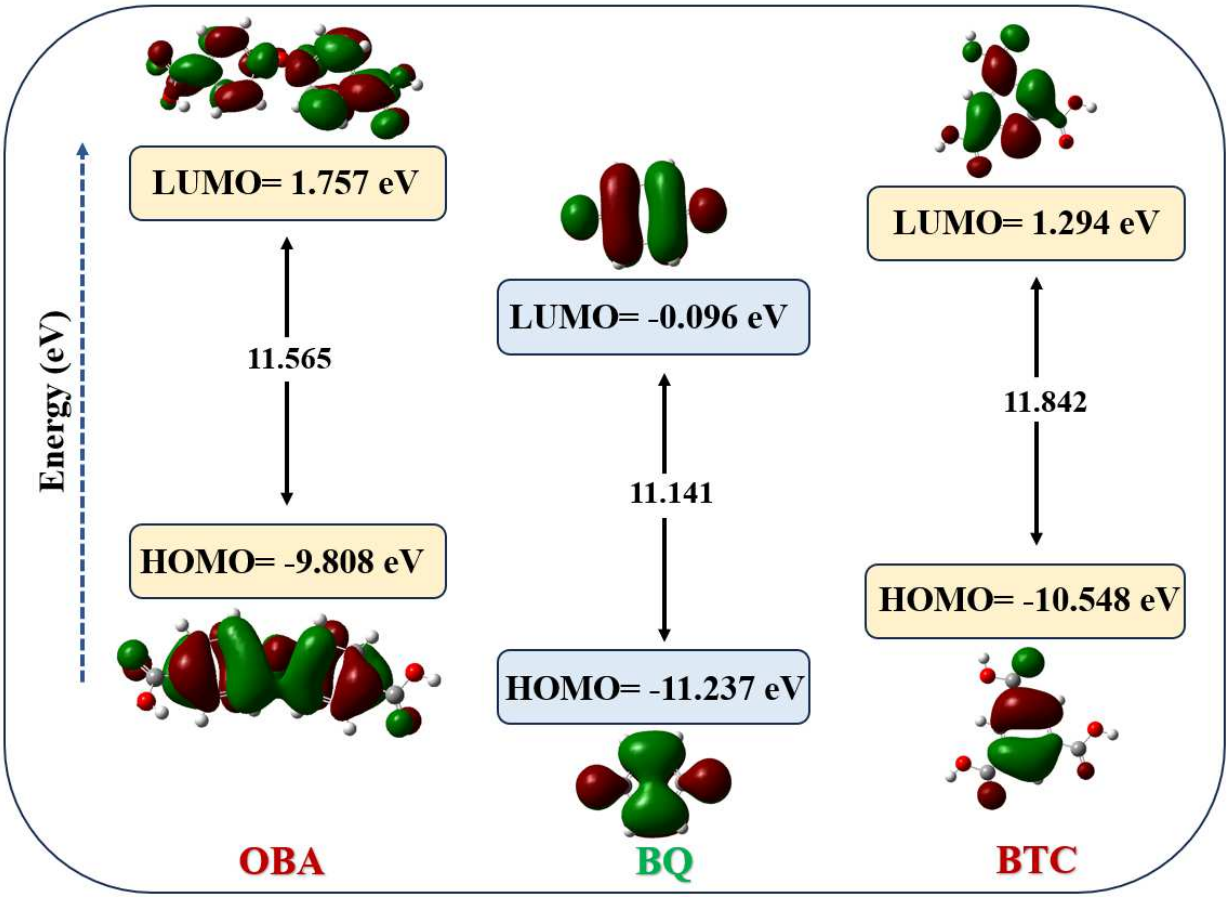

Figure 10. HOMO and LUMO plots of energies of BQ and MOF linkers (OBA, and BTC).

Supplementary information

Facile Layer Diffusion Technique for Synthesis of Terbium-Based Metal Organic Framework for Fluorometric Sensing of Hydroquinone

Gurdeep Singh [a], Rajpal Verma [a,c], Kirandeep Kaur [a], Deepika [a], Sanjay Kumar [b], Ashok Kumar Malik [a *]

[a] *Department of Chemistry, Punjabi University, Patiala-147002, Punjab, India*

[b] *Department of Chemistry, Multani Mal Modi College, Patiala-147001, Punjab, India*

[c] *Department of Chemistry, Dr. B. R. Ambedkar Govt. College Dabwali, Sirsa, Haryana, India*

[*]Corresponding author: malik_chem2002@yahoo.co.uk (A.K.M.)

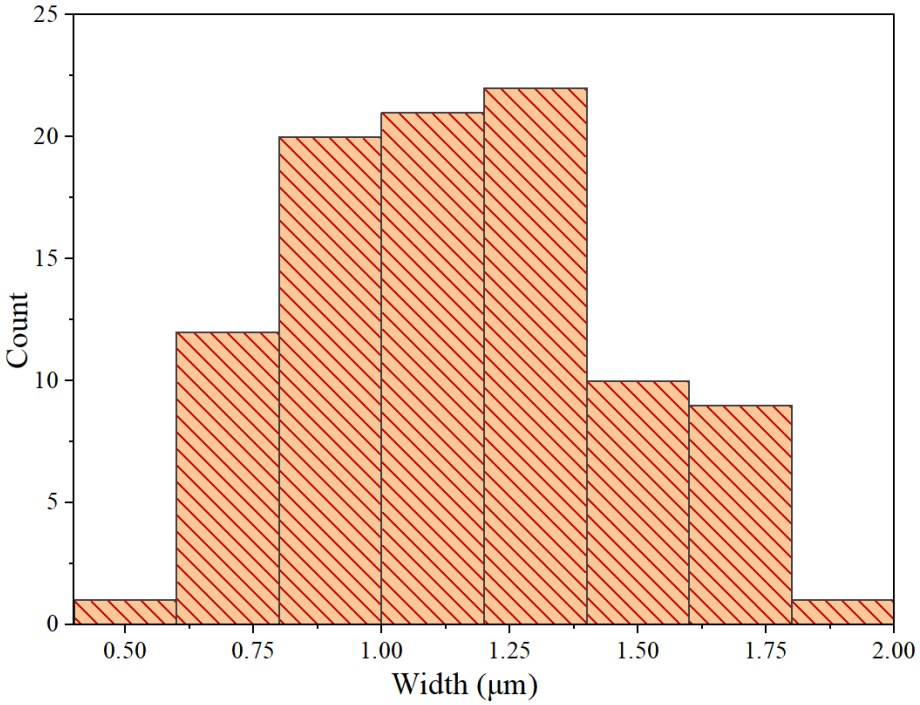

Figure S1. Evaluation of particle size distribution from FE-SEM micrographs.

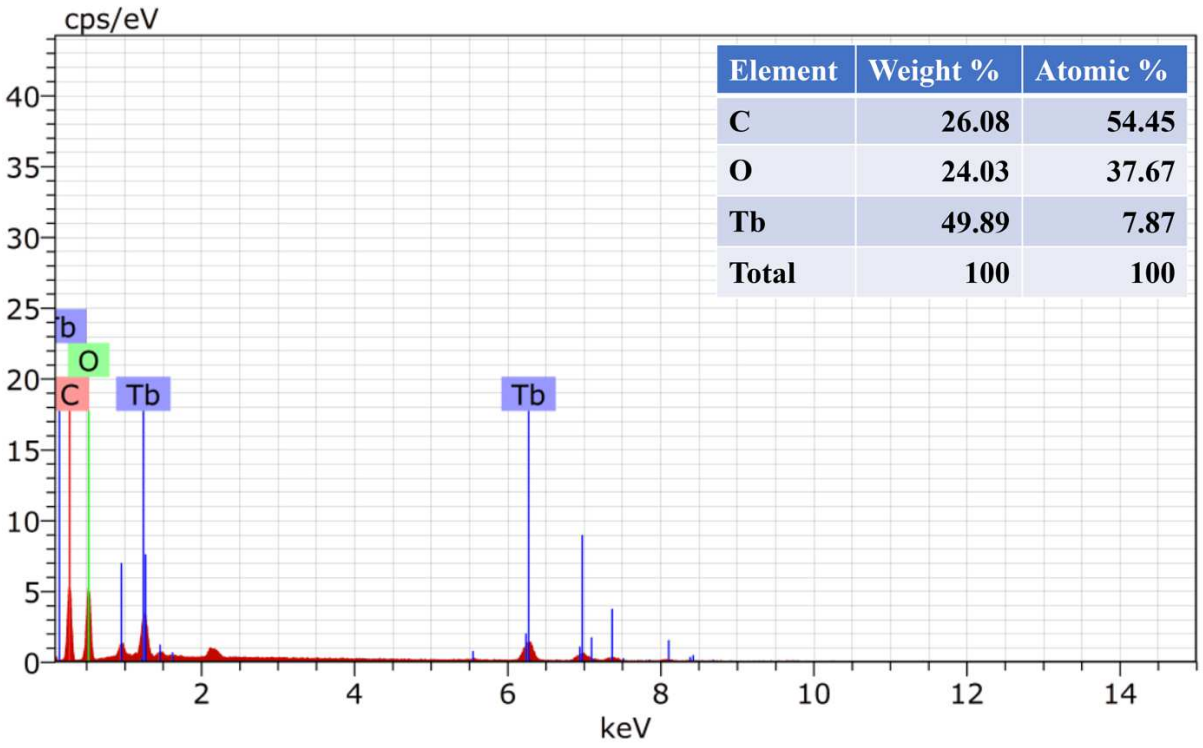

Figure S2. EDX spectra of **PUP-1**.

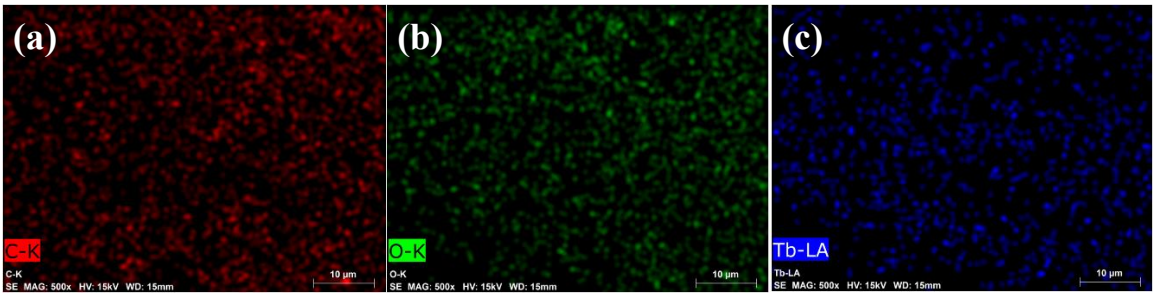

Figure S3. Elemental mapping of **PUP-1** showing **(a)** Carbon (C); **(b)** Oxygen (O); **(c)** Terbium (Tb).

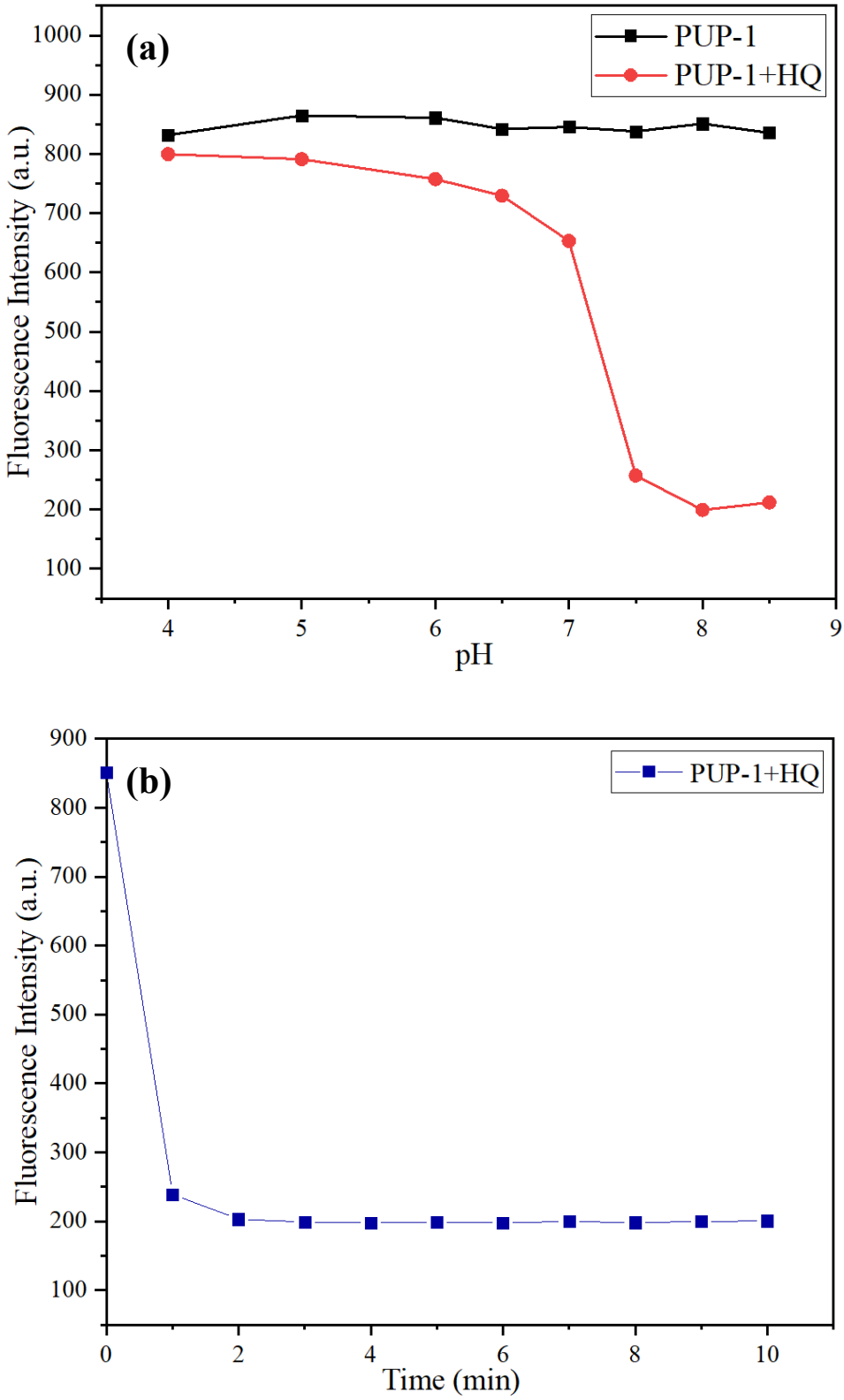

Figure S4. Optimizing parameters: (a) pH of solution and (b) time response.

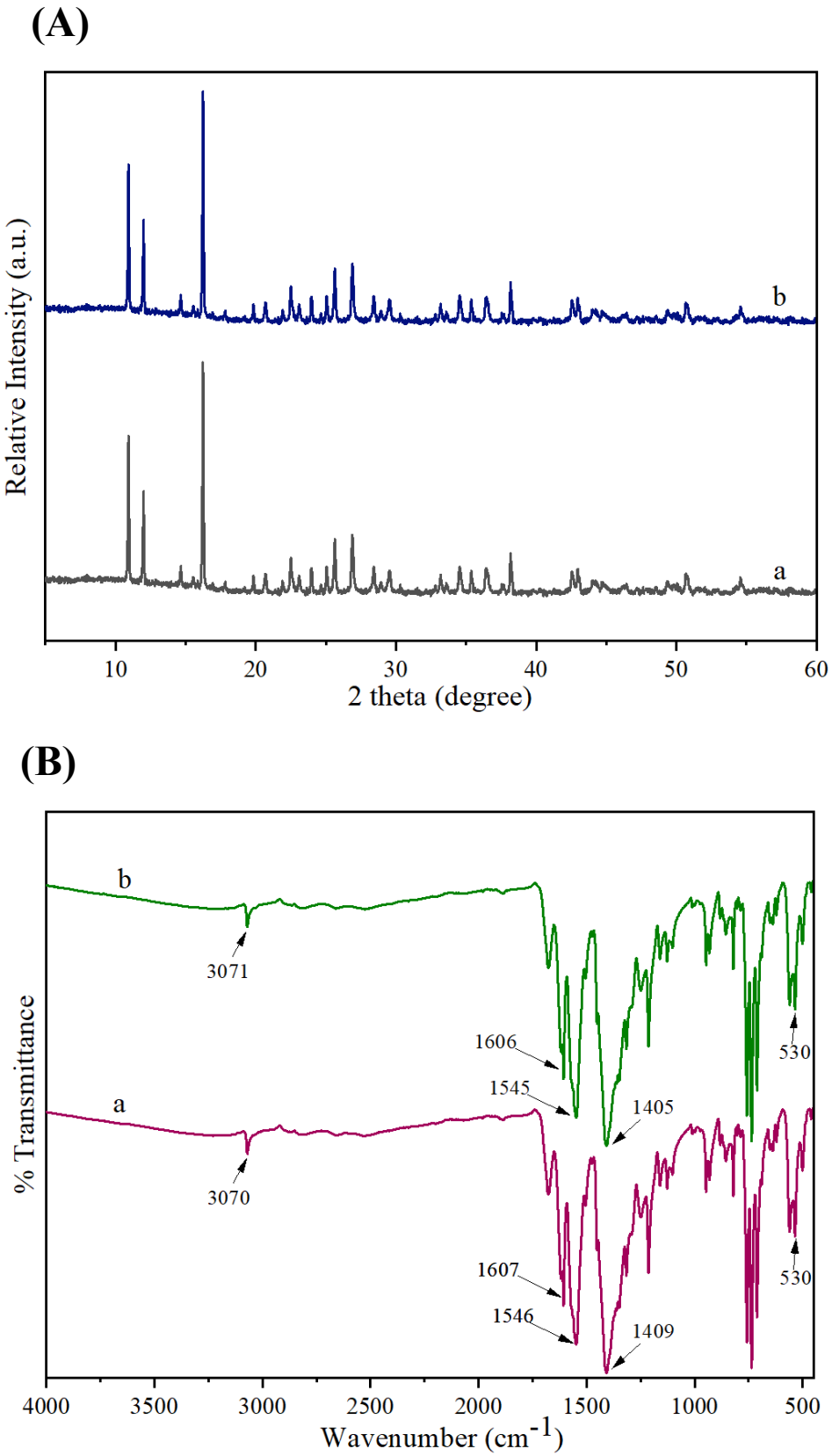

Figure S5. (**A**) The PXRD and (**B**) FT-IR of (**a**) fresh **PUP-1** and (**b**) **PUP-1** recovered after 3rd cycle.